

# High-temperature archeointensity measurements from Mesopotamia

Yves Gallet <sup>\*</sup>, Maxime Le Goff

*Equipe de Paléomagnétisme, Institut de Physique du Globe de Paris, 4 Place Jussieu, 75252 Paris Cedex 05, France*

Received 15 February 2005; received in revised form 27 September 2005; accepted 27 September 2005

Available online 28 November 2005

Editor: R.D. van der Hilst

## Abstract

We present new archeointensity results obtained from 127 potsherds and baked brick fragments dated from the last four millennia BC which were collected from different Syrian archeological excavations. High temperature magnetization measurements were carried out using a laboratory-built triaxial vibrating sample magnetometer (Triaxe), and ancient field intensity determinations were derived from the experimental procedure described by Le Goff and Gallet [Le Goff and Gallet. *Earth Planet. Sci. Lett.* 229 (2004) 31–43]. As some of the studied samples were previously analyzed using the classical Thellier and Thellier [Thellier and Thellier. *Ann. Geophys.* 15 (1959) 285–376] method revised by Coe [Coe. *J. Geophys. Res.* 72 (1967) 3247–3262], a comparison of the results is made from the two methods. The differences both at the fragment and site levels are mostly within  $\pm 5\%$ , which strengthens the validity of the experimental procedure developed for the Triaxe. The new data help to better constrain the geomagnetic field intensity variations in Mesopotamia during archeological times, with the probable occurrence of an archeomagnetic jerk around 2800–2600 BC.

© 2005 Elsevier B.V. All rights reserved.

*Keywords:* archeointensity; high temperature magnetization measurements; Triaxe; Thellier and Thellier method; Mesopotamia

## 1. Introduction

We recently developed a new three-axis vibrating sample magnetometer, herein called Triaxe, allowing continuous high-temperature and in-field magnetization measurements of small ( $\sim 0.75 \text{ cm}^3$ ) individual samples [1]. This equipment offers many possibilities for investigating rock magnetic properties at high temperature. As a first application, we proposed a completely automated experimental procedure that permits the rapid acquisition of arche- and paleointensity determinations corrected both for the thermo-remnant magnetization

(TRM) anisotropy and for the cooling rate dependence of TRM acquisition. Taking advantage of this new method, we analyze in the present study the natural remanent magnetization (NRM) of numerous (127) pottery and baked brick fragments from Syria archeologically dated from the last four millennia BC. Some of these fragments were previously studied by Genevey et al. [4] using the classical Thellier and Thellier [2] method revised by Coe [3] (hereafter referred as the TTC method), which allows one to make a detailed comparison between archeointensity values derived from the two different methodologies. The results obtained from a set of new dated-sites (i.e., groups of pottery or baked brick fragments of same age found together in the same archeological context) further provide new information on the variations of the geomagnetic field intensity in Mesopotamia over several millennia BC.

\* Corresponding author. Tel.: +33 1 4427 2432; fax: +33 1 4427 7463.

*E-mail addresses:* [gallet@ipgp.jussieu.fr](mailto:gallet@ipgp.jussieu.fr) (Y. Gallet), [legoff@ipgp.jussieu.fr](mailto:legoff@ipgp.jussieu.fr) (M. Le Goff).

## 2. High temperature archeointensity measurements

We briefly recall here the experimental procedure extensively described in Le Goff and Gallet [1] (Fig. 1). This procedure involves continuous magnetization measurements during heating and cooling. After a preliminary heating to  $T_1$  (generally 150–200 °C), a 1 cm-long/1 cm-diameter specimen is heated (demagnetized) in zero field to  $T_2$  (acquisition of the data  $M1(T)$ ;  $T_2$  is typically between 450 °C and 550 °C). It is then cooled in zero field to  $T_1$  and again heated to  $T_2$  in order to characterize the thermal variation between  $T_1$  and  $T_2$  of the magnetization fraction with unblocking temperature  $> T_2$  (acquisition of the data

$M3(T)$  during the heating). At  $T_2$ , a field of known intensity (Hlab) is applied and maintained while the specimen is cooled to  $T_1$ , which permits the acquisition of a laboratory TRM between  $T_2$  and  $T_1$ . Note that Hlab is applied so that the laboratory TRM is parallel to the NRM [1]. The field is next turned off and the specimen is again heated to  $T_2$  in zero field for demagnetizing the imparted laboratory TRM (acquisition of the data  $M5(T)$ ). The specimen is finally rapidly cooled from  $T_2$  to the room temperature.

This succession of steps made automatically by the Triaxe allows one to compute numerous values (every 5° between  $T_1$  and  $T_2$ ) of two ratios which both provide estimates of the ancient field intensity (Fig. 2). The first

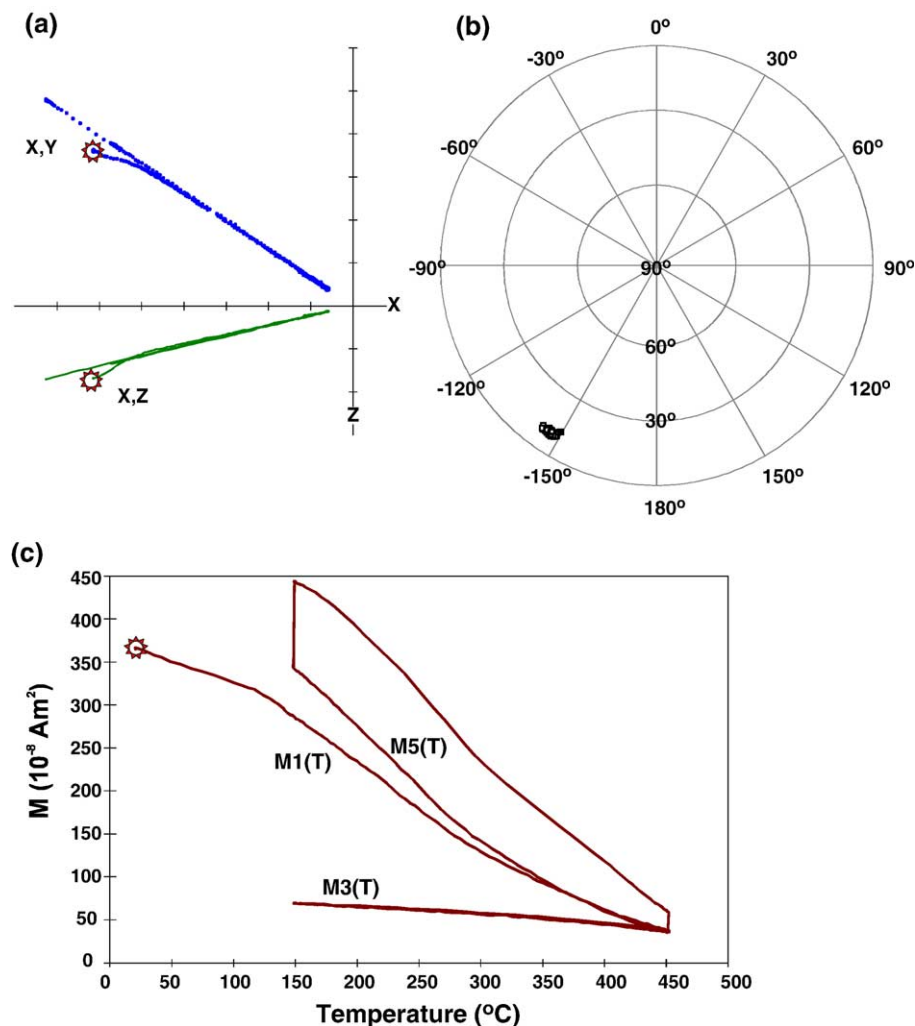


Fig. 1. Example of magnetization data acquired with the Triaxe allowing ancient field intensity determinations. The data are plotted both in orthogonal (a) and stereographic projections (b) in order to check the directional variations during heating, in particular during the demagnetization of the NRM (curve  $M1(T)$ ). In (c), the same data are reported as a function of temperature. The three curves  $M1(T)$ ,  $M3(T)$  and  $M5(T)$  are used for the intensity computations (see text and Le Goff and Gallet [1]). All data are reported in real time while they are continuously acquired.

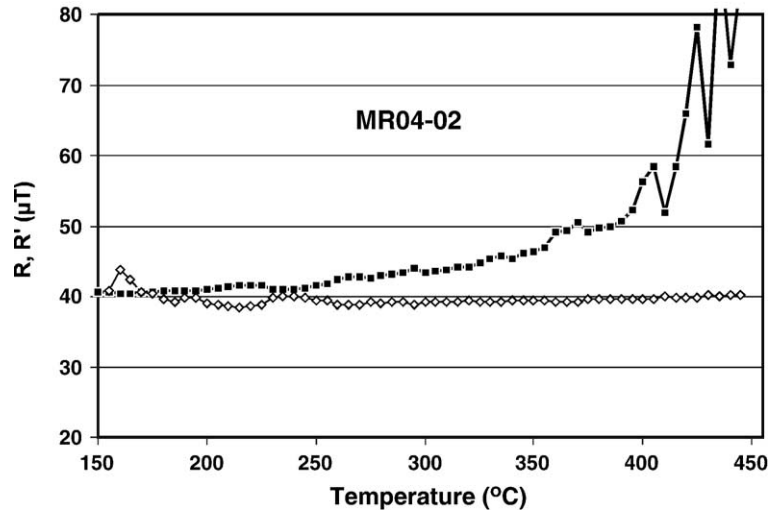


Fig. 2. Example of continuous ancient field intensity determinations deduced from the two ratios  $R(T_i)$  and  $R'(T_i)$  (curves with solid and open symbols, respectively). See text for explanations (see also Le Goff and Gallet [1]).

data set (hereafter called the  $R(T_i)$  data) is obtained by computing the ratio between the NRM and laboratory TRM fractions  $\Delta 1(T_i)$  and  $\Delta 5(T_i)$ , respectively) whose unblocking temperatures are between any temperature  $T_i$ , between  $T_1$  and  $T_2$ , and  $T_2$  (see also Boyd [5] and Tanaka et al. [6]).

$$R(T_i) = H_{lab} \cdot \Delta 1(T_i) / \Delta 5(T_i) \quad (1)$$

with

$$\Delta 1(T_i) = M1(T_i) - M3(T_i) \quad (2)$$

and

$$\Delta 5(T_i) = M5(T_i) - M3(T_i) \quad (3)$$

The second data set (hereafter called the  $R'(T_i)$  data) is derived from the ratio between the NRM and laboratory TRM fractions unblocked between  $T_1$  and any temperature  $T_i$  up to  $T_2$  ( $\Delta' 1(T_i)$  and  $\Delta' 5(T_i)$ , respectively). This option requires to make an approximation as the variations in spontaneous magnetization between  $T_1$  and  $T_i$  of the magnetization fraction with unblocking temperatures between  $T_i$  and  $T_2$  are not known. Le Goff and Gallet [1] found that, as a first approximation, these variations could be neglected. In this case, the  $R'(T_i)$  data are obtained from the formula:

$$R'(T_i) = H_{lab} \cdot \Delta' 1(T_i) / \Delta' 5(T_i) \quad (4)$$

with

$$\Delta' 1(T_i) = (M1(T_1) - M1(T_i)) - (M3(T_1) - M3(T_i)) \quad (5)$$

and

$$\Delta' 5(T_i) = (M5(T_1) - M5(T_i)) - (M3(T_1) - M3(T_i)) \quad (6)$$

In our previous study, we showed that the  $R(T_i)$  data are particularly sensitive to the cooling rate dependence of TRM acquisition (see for instance Fox et al. [7] and Genevey and Gallet [8]), while the  $R'(T_i)$  data are much less affected by this effect (the values being in all cases much more constant; Fig. 2). This difference in behavior between the  $R(T_i)$  and  $R'(T_i)$  data is due to the fact that the cooling rate effect essentially affects, at least in our archeological sample collection, the grains unblocked in the high temperature range. Our “best” estimate of the ancient field intensity corrected for the TRM anisotropy (as the laboratory TRM is parallel to the NRM) and for the cooling rate effect is obtained by averaging the  $R'(T_i)$  data within almost the entire  $T_1$ – $T_2$  temperature interval. Only the few first values close to  $T_1$  (over the ~20 first degrees) are eliminated because the magnetization fractions involved in  $R'(T_i)$  computations are then too small [1].

The measurements are carried out over a single but large temperature interval (generally 300 °C) which allows one to compare the unblocking spectrum of an important fraction of the NRM to that of the total experimental TRM. The main interest is that this makes the intensity determination very fast (~2 h and 10 min). We list below the selection criteria we used in this study for retaining only the most reliable results. These selection criteria were defined from

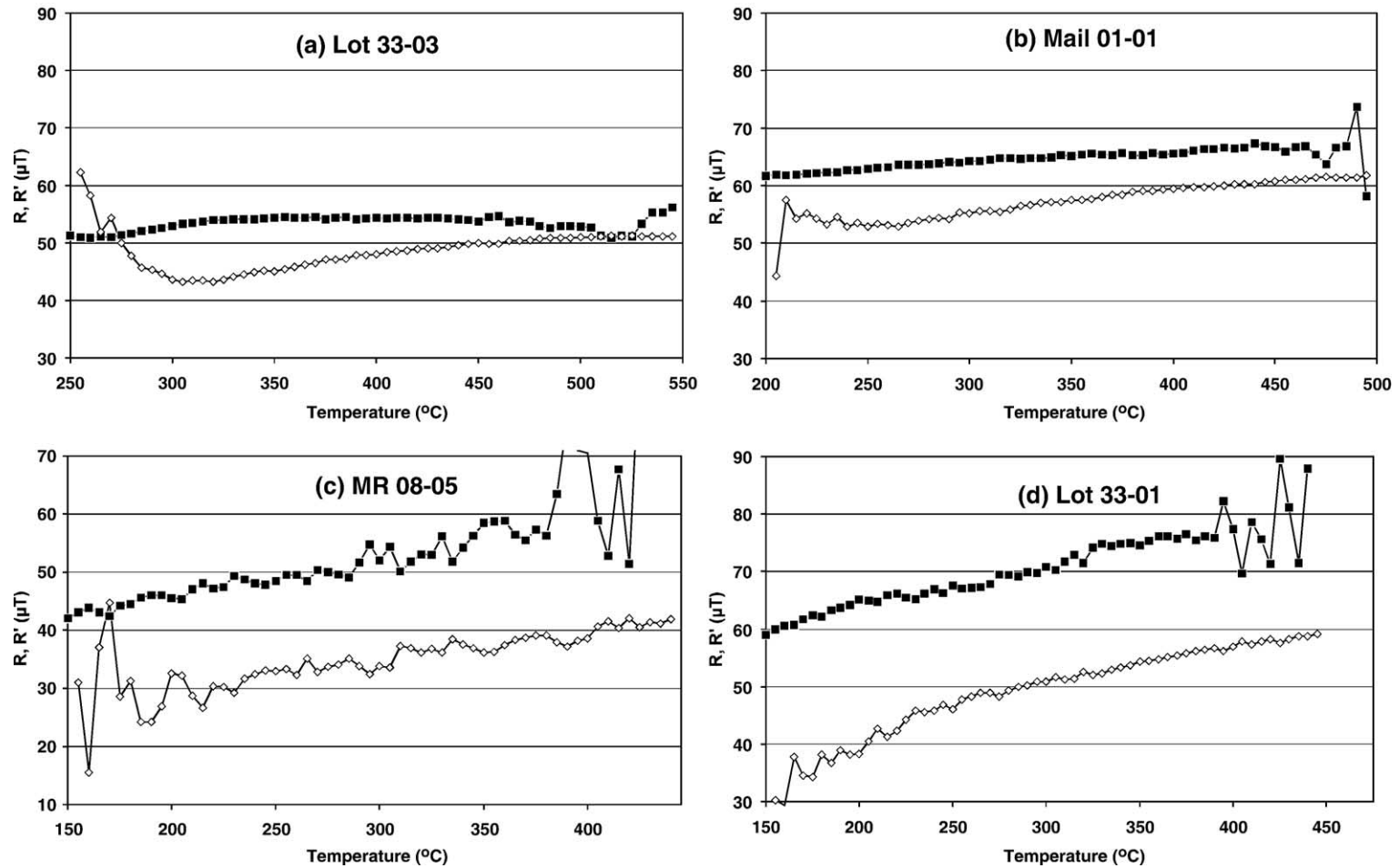


Fig. 3. Three examples of rejected Syrian samples because of unsatisfactory  $R(T_i)$  and/or  $R'(T_i)$  behaviors — (a), (c), (d). The behavior observed from a French potsherd is also shown for comparison in (b).

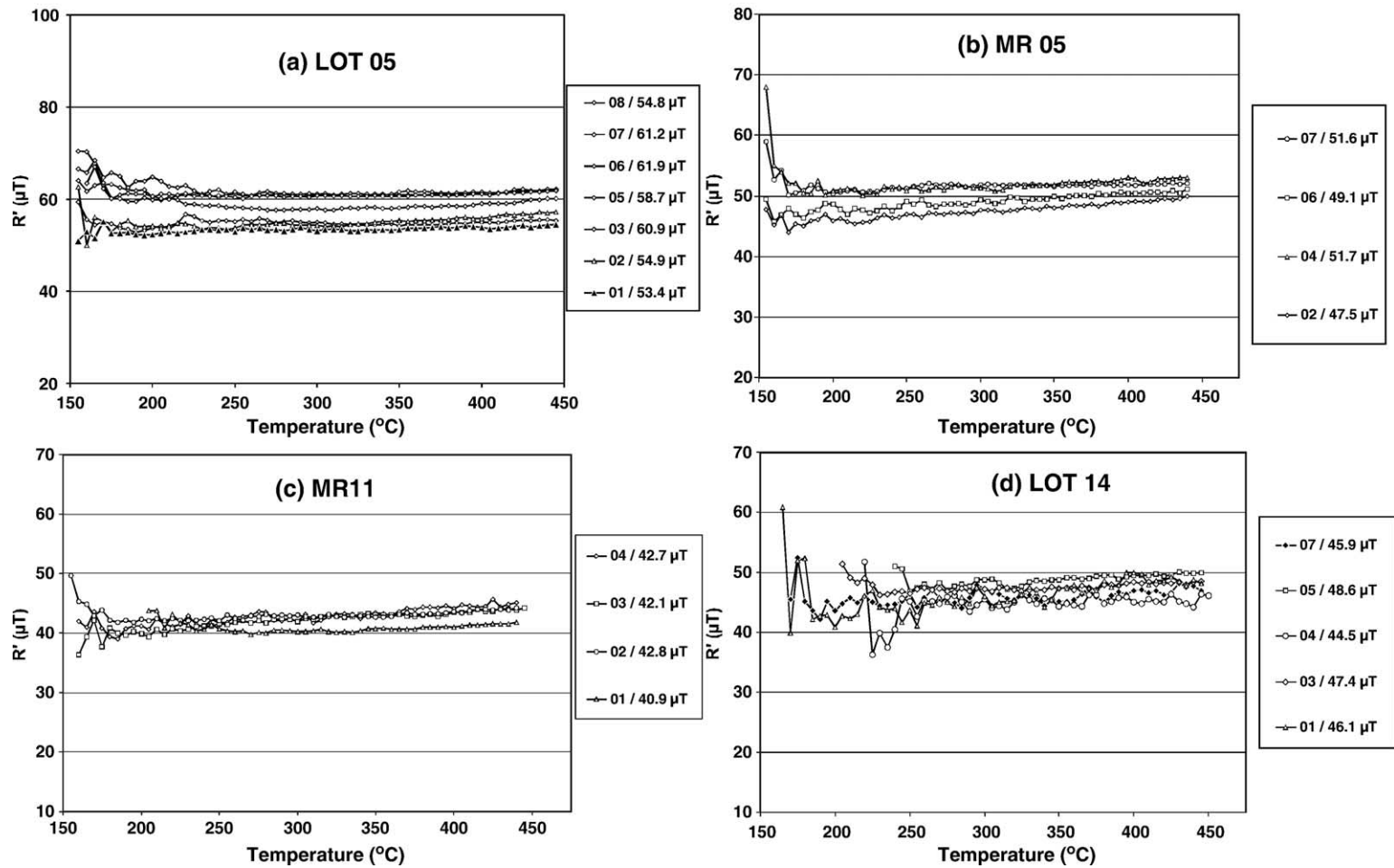
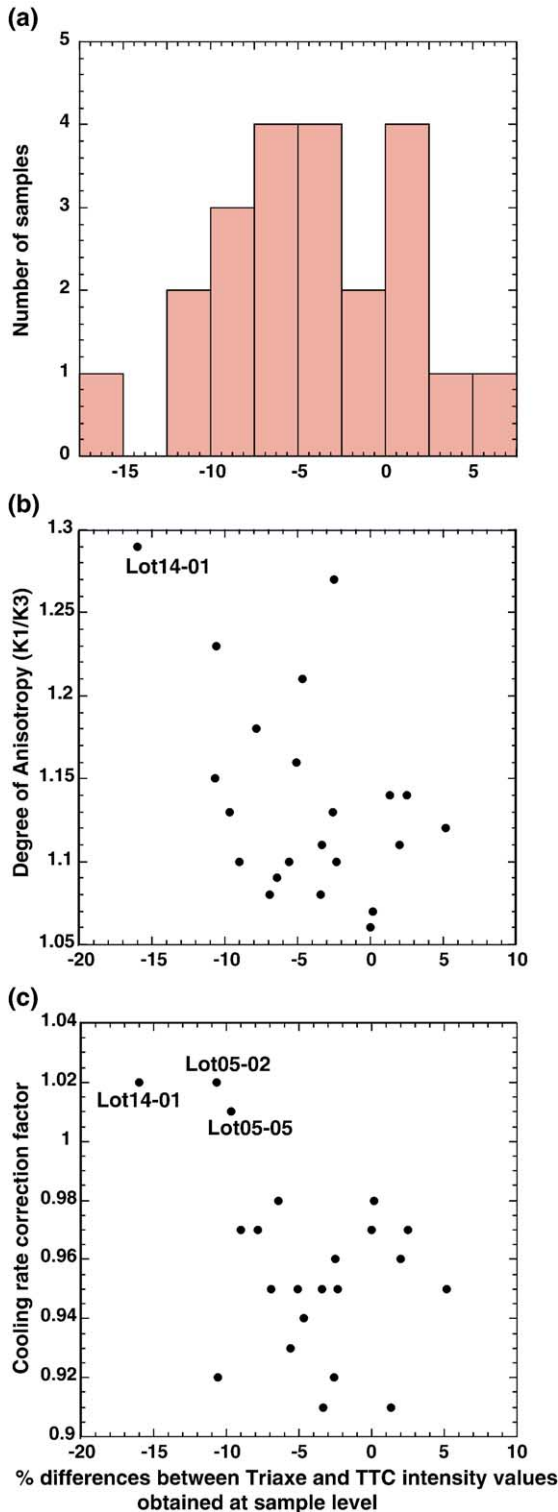


Fig. 4.  $R'(T_i)$  data obtained from four sites previously studied by Genevey et al. [4] using the TTC method. In our study, one sample per fragment was analyzed with the Triaxe providing each individual  $R'(T_i)$  curve, and each site comprises several fragments (=4).

numerous intensity measurements of pseudo-ancient NRM acquired in known thermal and laboratory-field conditions using thermally stabilized samples,

and subsequently analyzed using the experimental procedure described above.



- i) The magnetization must exhibit a single directional component through the entire temperature interval considered for archeointensity determination. The fact that there is only one magnetic component is controlled by looking at the directional data in real time both in orthogonal and stereographic projections (Fig. 1).
- ii) The magnetization fraction involved in the intensity determination between  $T_1$  and  $T_2$  must represent at least 50% of the magnetization fraction with unblocking temperatures larger than  $T_1$ .
- iii) The  $R(T_i)$  values must be continuously increasing or  $\sim$ constant from  $T_1$  to  $T_2$  (Fig. 2).
- iv) The  $R'(T_i)$  values must be nearly straight (Fig. 2). In most samples however, the  $R'(T_i)$  data are slightly increasing, which defines a slope, through the temperature interval of analysis. The lower the slope of the  $R'(T_i)$  data between  $T_1$  and  $T_2$ , the better the intensity estimate. Here we compute the slope from the ratio  $(R'(T_2) - R'(T_1)) / (\text{mean } R'(T_i) \text{ data})$ , expressed in %, after fitting the  $R'(T_i)$  data with a linear trend. We reject the specimen if the slope of the  $R'(T_i)$  data is  $> 15\%$ . Note that these smoothed  $R'(T_i)$  data are only considered for slope computations.
- v) For each dated site, we analyze specimens taken from different pottery and/or brick fragments (one specimen per fragment). The site mean intensity is computed from a number  $> 3$  of independent results obtained at the fragment level, all having the same weight in this computation. In addition to all previous criteria relying on the magnetic behavior observed for each specimen, this approach further minimizes the possibility for a systematic bias at the site level due to alteration and especially helps to control the homogeneity in age of the studied fragments. It is worth pointing out that this would not be possible if the definition of the dated site was a set of several specimens collected from the same potsherd or brick fragment.

Fig. 5. Analysis of the differences between the intensity values obtained at the fragment level from the TTC and Triaxe methods (expressed in %, and relative to the TTC results obtained by Genevey et al. [4]). The differences are reported in a histogram in (a), and they are also plotted as a function of the degree of TRM anisotropy (b) and of the cooling rate correction factor (c) determined for each sample by Genevey et al. [4].

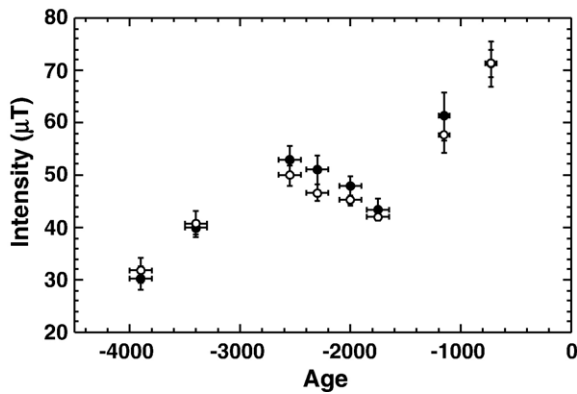


Fig. 6. Mean intensity values as a function of time obtained at the site level from the Triaxe (open symbols) and TTC (solid symbols) methods.

Three examples of rejected Mesopotamian results are shown in Fig. 3a,c,d. They failed at least one, but mostly several criteria, despite the fact that the demagnetization of the NRM is univectorial. These examples illustrate typical complex behaviors that were never observed in thermally stabilized archeological and volcanic samples. For potsherd Lot33-03 (Fig. 3a), the  $R(T_i)$  data

start to increase before to slightly decrease toward the end of the temperature interval of analysis whereas the  $R'(T_i)$  data strongly vary throughout the entire temperature interval. This behavior is similar to the one shown in Fig. 7 of our previous study [1] obtained from a French Dark Middle Age potsherd, and is again observed in another French potsherd but dated from the first Iron Age (Fig. 3b). Samples MR08-05 (Fig. 3c) and Lot33-01 (Fig. 3d) illustrate another case where the  $R(T_i)$  and  $R'(T_i)$  data display curves which are roughly parallel, with strongly increasing  $R'(T_i)$  data, through the temperature interval of analysis.

### 3. Comparison between high-temperature and room-temperature archeointensity determinations

We have pursued the investigation of the collection of archeological samples assembled during the Genevey's thesis [9] (see Genevey et al. [4]). The comparison between the results derived from the Triaxe procedure and those obtained by Genevey et al. [4] using the TTC method is performed at two different levels: 1) at the fragment level (i.e., the same fragments

Table 1  
Name, location and age of the new studied Syrian sites of pottery and baked brick fragments

Archeological sites	Lat (°N)	Long (°E)	Name of groups	Nature of fragments (*)	Associated culture, period, empire	Age	References
Mashnaqa	36.3	40.8	MAS 02	C	Early Dynastic II	2800–2600 BC	[10]
Mari	34.5	40.9	Lot 24	C	Early Dynastic I	3000–2800 BC	[12]
			MR 14	B	Early Dynastic III	2650–2450 BC	[13]
			MR 15	B	Dynasty of Ur III	2100–1900 BC	[13]
			MR 03	B	Dynasty of Ur III	2100–1900 BC	[13]
			MR 04	B	Dynasty of Ur III	2100–1900 BC	[13]
			MR 08	B		1850–1650 BC	[13]
Sheikh Hamad	35.8	40.9	Lot 27	C	Middle Assyrian	1300–1200 BC	[15]
			Lot 31	C	Neo-Assyrian	600–550 BC	[15]
Tell Masaikh	35.0	40.6	Lot 28	C	Neo-Assyrian	750–700 BC	[14]
			Lot 29	C	Neo-Assyrian	700–600 BC	[14]
Shaara	32.7	36.6	Lot 33	C		200–100 BC	[16]

(\*): C for Ceramics and B for Bricks.

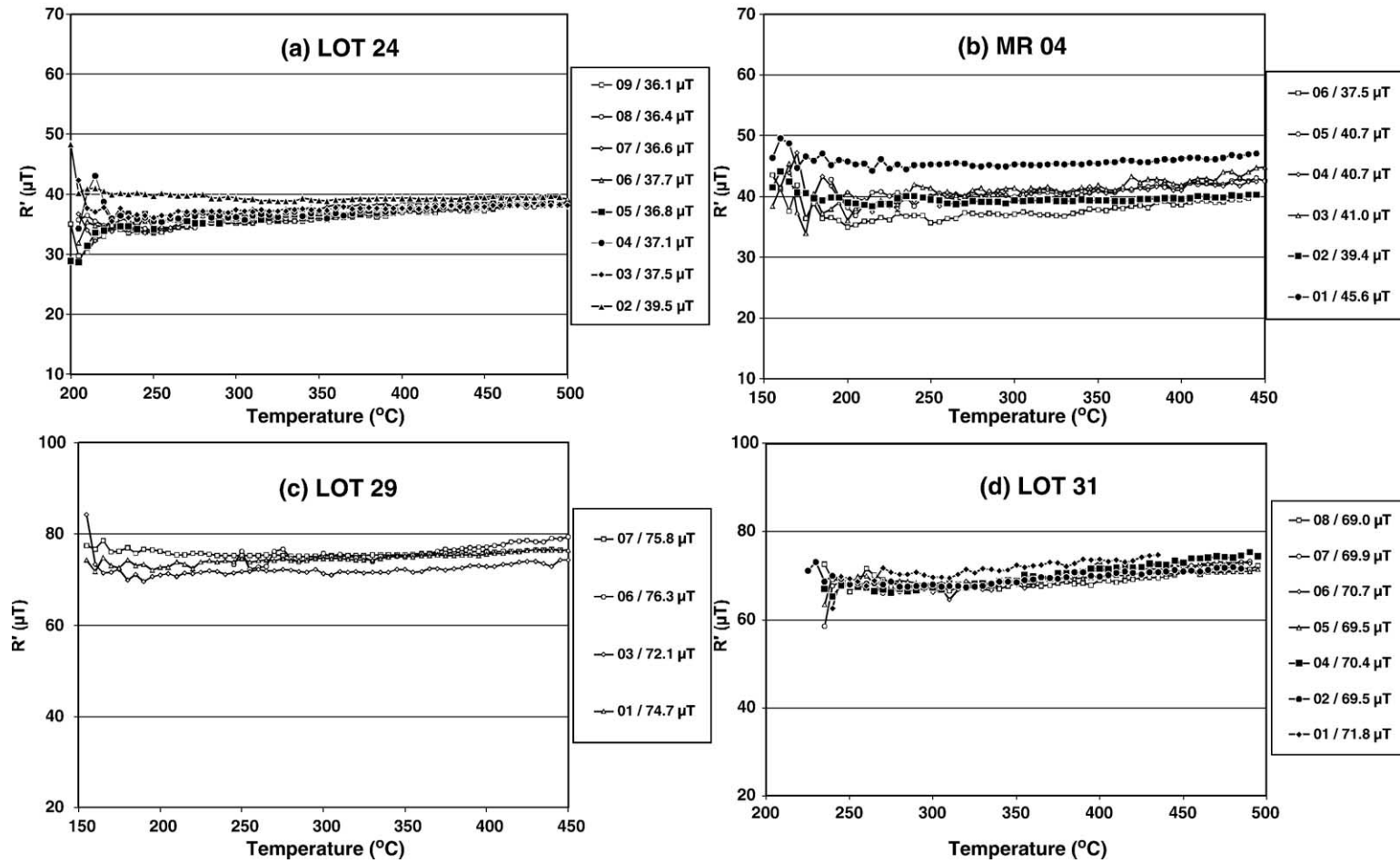


Fig. 7.  $R'(T_i)$  data obtained from four new Syrian sites.

were studied). This concerns 36 pottery and brick fragments, 10 having failed in providing TTC values; and 2) at the dated-site level (i.e., the same groups of fragments found in the same archeological context were studied, including some additional fragments which were not investigated by Genevey et al. [4]). This comprises eight dated-sites and 11 newly investigated fragments. As a whole, the comparison relies on 47 fragments analyzed with the Triaxe (Table 2).

The  $R'(T_i)$  data obtained from four sites are shown in Fig. 4. From these plots, it is quite easy to judge the overall quality of the data, with a direct information on the dispersion both at the sample level (the behavior of each  $R'(T_i)$  curve) and at the site level (the comparison between the different  $R'(T_i)$  curves from the same site). Ten samples (~21% of the collection) were rejected because they failed at least one of our selection criteria (principally those concerning the univectorial NRM demagnetization behavior and the slope of the  $R'(T_i)$  data). Among the ten common fragments rejected by Genevey et al. [4], six are again rejected in our study (Table 2). The four others do not appear problematic, being very close to the values obtained from their respective sites. In particular, potsherd Lot17-19 was rejected by Genevey et al. [4] because the two studied specimens yielded TTC intensity values that differ by more than 5%. However, we could not perform this test because only a single specimen per potsherd was analyzed with the Triaxe. The 5% coherence criterion [4] was satisfied for potsherd MR05-06, but the latter was rejected because a moderate alteration was detected during cooling rate experiments conducted on a third specimen. In contrast, four fragments retained by Genevey et al. [4] were rejected when analyzed with the Triaxe. We consider that the differences above are due to the strict application of severe selection criteria. The comparison at the fragment level between TTC and Triaxe accepted values is possible only for 22 samples. The differences (Triaxe intensity – TTC intensity)/TTC Intensity expressed in % are comprised between –16.0% and +5.2% (Table 2, Fig. 5a). In a large proportion, the intensity results obtained using the Triaxe are smaller than those obtained from the TTC method (with a mean difference of  $-4.3 \pm 5.1\%$ ).

For deciphering the origin of these differences, we reported them both as a function of the degree of TRM anisotropy ( $K_{\max}/K_{\min}$ ; Fig. 5b) and of the cooling rate correction factor (Fig. 5c) determined by Genevey et al. [4] for each studied sample. We recall that Genevey et al. [4] (see also Genevey and Gallet [8]) estimated the cooling rate correction factors from the ratio between the TRM acquired for the same temperature interval

(generally from  $\sim 450$  °C to room temperature) at rapid ( $\sim 30$  min) and slow ( $\sim 10$  or 30 h) cooling rates. The two figures show that the differences observed between the two intensity data sets are controlled neither by the degree of TRM anisotropy nor by the cooling rate effect. Three samples (Lot14-01, Lot05-02 and Lot05-05) however appear to lie outside of the normal distribution seen in Fig. 5c. They all have a cooling rate correction factor larger than 1 (i.e., the intensity value increases after the correction for the cooling rate dependence of TRM acquisition; Table 2), which is a rare characteristic in the sample collection studied by Genevey et al. [4], and their intensity differences are among the largest: –16.0%, –10.7% and –9.7%, respectively (Table 2). We also remark that sample Lot14-01, which reveals the largest difference between the Triaxe and TTC intensity values, possesses the largest degree of anisotropy (1.29; Fig. 5b), and its TTC intensity value significantly differs from the other data obtained from the same site (Table 2). The TTC values obtained from these three samples most probably suffer from some experimental uncertainties. Excluding these problematic samples, the averaged difference between the Triaxe and TTC intensity values decreases to  $-3.1 \pm 4.2\%$ . Such a difference therefore does not cast doubt on the validity of the experimental procedure developed for the Triaxe.

The reliability of the Triaxe intensity data is further strengthened by the comparison between the Triaxe and TTC results obtained at the site level. The average of the site-mean intensity differences is  $-2.8 \pm 4.5\%$ . Excluding the three problematic samples discussed above has the consequence that a mean intensity value cannot be computed for site Lot05 because of insufficient

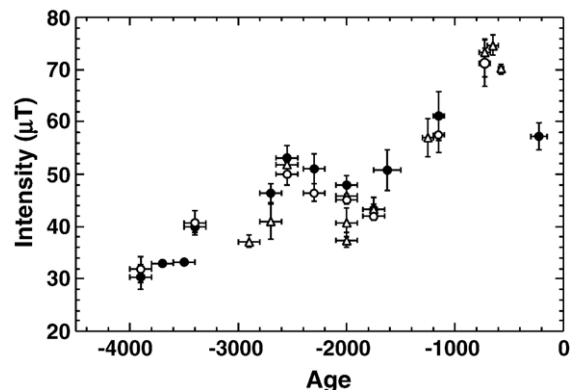


Fig. 8. All site-mean intensity values obtained in this study (open symbols) and by Genevey et al. [4] (solid symbols) for the past four millennia BC in Syria. Solid and open circles indicate that exactly the same sites were analyzed using the two methods, whereas the Triaxe means obtained from new sites are indicated by open triangles. All results were derived at the site of Mari ( $\lambda = 34.5^\circ\text{N}$ ,  $\phi = 40.9^\circ\text{E}$ ).



MR 02	Mari	2100–1900 BC									47.9 ± 1.9	45.2 ± 0.9	3	–5.7%
			MR 02-01											
			MR 02-02	150–450	50	58	14	45.5	48.2	0.2	–5.6%			
			MR 02-03	150–450	50			Rejected	50.4	0.5				
			MR 02-04	150–450	50			Rejected	Rejected					
			MR 02-05	300–450	50			Rejected	46	0.2				
			MR 02-06	150–450	50	65	4	45.8	46.9	0.2	–2.3%			
			MR 02-07	150–450	50	73	5	44.2						
MR 11	Mari	1850–1650 BC									43.4 ± 2.2	42.1 ± 0.9	4	–2.9%
			MR 11-01	200–500	50	76	2	40.9	40.9	0.2	0.0%			
			MR 11-02	150–450	40	73	4	42.8	44.3	0.2	–3.4%			
			MR 11-03	150–450	40	53	12	42.1	45	0.4	–6.4%			
			MR 11-04	150–450	40	63	12	42.7	Rejected					
Lot 05	Tell Mashtale	1200–1100 BC									61.5 ± 4.7	58.0 ± 3.5	7	–5.7%
			Lot 05-01	150–450	60	90	3	53.4	54.8	0.6	–2.6%			
			Lot 05-02	150–450	60	84	6	54.9	61.5	0.2	–10.7%			
			Lot 05-03	150–450	60	81	1	60.9						
			Lot 05-04	150–450	60			Rejected	Rejected					
			Lot 05-05	150–450	60	71	0	58.7	65	0.6	–9.7%			
			Lot 05-06	150–450	60	62	–3	61.9						
			Lot 05-07	150–450	60	81	0	61.2	64.5	0.6	–5.1%			
			Lot 05-08	150–450	60	79	1	54.8						
TM 01	Tell Masaikh	750–700 BC									71.6 ± 4.3	71.7 ± 2.7	6	0.1%
			TM 01-01											
			TM 01-02	150–450	70	83	9	70.6	67.1	0.2	5.2%			
			TM 01-03	150–450	70	73	7	71.2	70.3	0.3	1.3%			
			TM 01-04	150–450	70	80	10	70.2						
			TM 01-05	150–450	70	55	10	77.1	75.6	1.6	2.0%			
			TM 01-06	150–450	70	71	12	70.6	76.6	0.3	–7.8%			
			TM 01-07	150–450	70	81	7	70.2	68.5	0.2	2.5%			

Temp. int., temperature interval (in °C) of intensity determination; Lab H., laboratory field used for TRM acquisition; NRM  $T_1$  (%), fraction of NRM involved from  $T_1$  in intensity determination; Slope  $R'$  (%), slope of the  $R'(T_i)$  data within the temperature interval of analysis (see text for further explanation); Int. Triaxe, intensity value in  $\mu\text{T}$  derived per fragment from the Triaxe (this study); TTC fragment, mean intensity value determined at the fragment level from two specimens by Genevey et al. [4] using the TTC method; SD (2 spec.), standard deviation in  $\mu\text{T}$  of the TTC mean intensity value determined at the fragment level; Sample dif., difference expressed in % between the Triaxe and TTC intensity values obtained at the fragment level; TTC site intensity, mean TTC value in  $\mu\text{T}$  obtained at the site level and its standard deviation; Triaxe site intensity, mean Triaxe intensity value in  $\mu\text{T}$  obtained at the site level and its standard deviation; Nb, number of data used for the computation of the mean Triaxe intensity value; Site dif., difference expressed in % between the mean TTC and Triaxe intensity values determined at the site level.

Table 3  
Triaxe archeointensity results obtained from new Syrian dated-sites

Site	Location	Age	Sample	Temp. inter.	Lab H.	NRM $T_1$ (%)	Slope $R'$ (%)	Int. Triaxe	Mean int.	Nb samples
Lot 24	Mari	3000–2800 BC							$37.2 \pm 1.1$	8
			Lot 24-01	200–500	40			Rejected		
			Lot 24-02	200–500	40	84	–1	39.5		
			Lot 24-03	200–500	40	85	5	37.5		
			Lot 24-04	200–500	40	86	9	37.1		
			Lot 24-05	200–500	40	85	13	36.8		
			Lot 24-06	200–500	40	91	13	37.7		
			Lot 24-07	200–500	40	88	15	36.6		
			Lot 24-08	200–500	40	90	13	36.4		
Lot 24-09	200–500	40	88	14	36.1					
MAS 02	Mashnaqa	2800–2600 BC							$40.9 \pm 3.4$	4
			MAS 02-01	150–450	50	60	9	45.9		
			MAS 02-02	150–450	50	73	15	38.8		
			MAS 02-03	150–450	50	93	3	39.1		
			MAS 02-04	150–450	50			Rejected		
			MAS 02-05	150–450	40	78	6	39.6		
			MAS 02-06	200–450	40			Rejected		
MAS 02-07	230–450	40			Rejected					
MR 14	Mari	2650–2450 BC							$51.9 \pm 0.4$	5
			MR 14-01	150–450	50	76	7	52		
			MR 14-02	300–450	50	60	7	51.3		
			MR 14-03	150–450	50	58	5	52.5		
			MR 14-04	150–500	50	52	8	52.1		
MR 14-05	150–500	50	55	12	1.7					
MR 15	Mari	2100–1900 BC							$45.9 \pm 1.5$	6
			MR 15-01	150–450	50	68	3	45.9		
			MR 15-02	150–450	50	74	6	47.8		
			MR 15-03	150–450	50	73	4	45.1		
			MR 15-04	150–450	50	66	5	44.2		
			MR 15-05	150–450	50	75	6	47.6		
MR 15-06	150–450	50	82	1	44.6					
MR 04	Mari ville 3	2100–1900 BC							$40.8 \pm 2.7$	6
			MR 04-01	150–450	40	64	2	45.6		
			MR 04-02	150–450	50	76	1	39.4		
			MR 04-03	150–450	50	53	13	41.0		
			MR 04-04	150–450	40	67	7	40.7		
			MR 04-05	190–450	50	61	10	40.7		
MR 04-06	150–450	40	55	11	37.5					
MR 03	Mari ville 3	2100–1900 BC							$37.4 \pm 1.4$	6
			MR 03-01	150–450	50	73	4	37.4		
			MR 03-02	150–450	40	74	9	39.8		
			MR 03-03	150–450	40			Rejected		
			MR 03-05	150–450	40	56	15	36.9		
			MR 03-06	150–450	40	64	7	36.8		
			MR 03-07	150–450	40	75	4	36		
MR 08	Mari	1850–1650 BC							$43.4 \pm 0.9$	4
			MR 08-01	150–500	40	53	6	43.6		
			MR 08-02	230–450	40			Rejected		
			MR 08-03	150–450	40	63	15	44.6		
			MR 08-04	150–450	40	65	6	43.1		
			MR 08-05	150–450	40			Rejected		
MR 08-06	150–450	40	52	13	42.4					

Table 3 (continued)

Site	Location	Age	Sample	Temp. inter.	Lab H.	NRM $T_1$ (%)	Slope $R'$ (%)	Int. Triaxe	Mean int.	Nb samples
Lot 27	Sh. Hamad	1300–1200	Lot 27-01	150–450	60			Rejected	$57.1 \pm 3.6$	4
			Lot 27-02	150–450	60	76	15	55.6		
			Lot 27-03	200–450	60	54	14	54.5		
			Lot 27-04	150–450	60	64	0	61.2		
			Lot 27-05	150–450	60			Rejected		
			Lot 27-06	150–450	60			Rejected		
			Lot 27-07	Magnetization too weak						
Lot 28	Tell Masaikh	750–700 BC	Lot 28-01	150–450	70	75	5	75.9	$73.4 \pm 2.5$	8
			Lot 28-02	150–450	70	83	7	70		
			Lot 28-03	250–450	70	59	15	71		
			Lot 28-04	150–450	70	82	3	75.1		
			Lot 28-05	220–450	70	61	13	70.5		
			Lot 28-06	150–450	70	64	5	73.4		
			Lot 28-07	150–450	70	71	8	75		
			Lot 28-08	150–450	70	73	6	76.2		
Lot 29	Tell Masaikh	700–600 BC	Lot 29-01	150–450	70	84	5	74.7	$74.7 \pm 1.9$	4
			Lot 29-02	150–450	70			Rejected		
			Lot 29-03	150–450	70	74	4	72.1		
			Lot 29-04	150–450	70			Rejected		
			Lot 29-05	150–450	70			Rejected		
			Lot 29-06	250–450	70	58	10	76.3		
			Lot 29-07	150–450	70	90	1	75.8		
Lot 31	Sh. Hamad	600–550 BC	Lot 31-01	230–450	70	84	12	71.8	$70.1 \pm 0.9$	7
			Lot 31-02	350–500	70	96	7	69.5		
			Lot 31-03	225–500	70			Rejected		
			Lot 31-04	275–500	70	86	14	70.4		
			Lot 31-05	225–500	70	90	5	69.5		
			Lot 31-06	300–500	70	81	13	70.7		
			Lot 31-07	225–500	70	92	11	69.9		
			Lot 31-08	225–500	70	85	6	69		
Lot 33	Shaara	200–100 BC	Lot 33-01	250–450	60			Rejected		1
			Lot 33-02	200–500	60			Rejected		
			Lot 33-03	330–550	60			Rejected		
			Lot 33-04	225–525	50	90	14	51.6		
			Lot 33-05	285–525	50			Rejected		
			Lot 33-06	370–525	50			Rejected		

Same conventions as in Table 2.

number of data ( $N=2$ ). For the remaining sites, the mean difference is  $-2.0 \pm 4.2\%$ . The mean intensity values are finally reported in Fig. 6 as a function of age. This figure shows that for each case the mean intensity values obtained from the same site using the different methods agree with one another within their error bars.

#### 4. Discussion

From the previous results, we consider that our experimental procedure using the Triaxe provides in  $\sim 2$  h an intensity value from one sample which is as reliable as

data obtained from the TTC method with stringent selection criteria and corrected as precisely as possible for the anisotropy of TRM and for the cooling rate dependence of TRM acquisition [4,8]. We then obtained additional archeointensity results from 12 new dated sites collected from different Syrian archeological excavations (Mashnaqa, Mari, Tell Masaikh, Sheikh Hamad and Shaara; Table 1 [10–16]). This concerns 80 fragments whose results are reported in Table 3. The  $R'(T_i)$  data obtained from 4 sites are shown in Fig. 7. Nineteen samples failed our selection criteria (24%), which again demonstrates the overall good suitability of the Meso-

potamian pottery and brick fragments for archeointensity studies [4]. This is likely due to a combination of several favorable parameters such as the type of clays, the preparation for making these archeological objects, the firing conditions and the region's dry climate. However, the site from Shaara (Lot33) had to be rejected because only one fragment provided a satisfactory result (against 5 rejected data; Fig. 3b,c and Table 3).

Fig. 8 displays the mean intensity values previously obtained by Genevey et al. [4] together with the new ones obtained using the Triaxe. Altogether these data provide a description of the changes in geomagnetic field intensity in the Middle East during the last four millennia BC. The new data, although they bring more details on these variations, do not modify the field behavior discussed in Genevey et al. [4] (see comparisons with other archeointensity data sets in the latter study). It is however of interest to recall the rapid and important intensity fluctuations between ~2000 and 0 BC, with an intensity increase by a factor ~1.8 between ~2000 and ~750 BC. There is a very high intensity maximum during the first half of the first millennium BC, which was associated with an archeomagnetic jerk by Gallet et al. [17]. The new data strengthen the possibility that a sharp intensity increase happened around 2800–2600 BC (Fig. 8; see also Genevey et al. [4]): the latter could reveal the occurrence of another archeomagnetic jerk, perhaps also detected by Snowball and Sandgren [18] from lake sediments in Sweden.

The agreement between intensity results obtained from sites archeologically dated of the same age is particularly satisfactory in three cases (Tables 2 and 3). This concerns for instance the new site Lot28 from Tell Masaikh consisting of potsherds found directly overlying the baked brick pavement that constitutes site TM01 [4]. The site mean difference between the two (Triaxe and TTC, respectively) intensity values is only 2.5%. The agreement is also almost perfect between sites MR08 and MR11 collected from two different pavements dated at the end of city 3 of Mari (difference of 0.1%) and between sites MR14 and MR05 (baked brick fragments from a water conduct and from a pavement), both dated at the beginning of city 2 of Mari, with a mean intensity difference of –2.0%. However, the new Triaxe data illustrate in two cases some limitations due to the dating precision of the studied sites. The first case concerns two sites collected from two different excavations (Mari and Mashnaqa [10,12]) and dated between 2800 and 2600 BC (Fig. 8). These two sites provide significantly different mean intensity values, which indicates that these two sites do not have the same age within the same age bracket given by the archeologists (i.e., based

on the archeological context linked to a cultural settlement). According to the field intensity variations, the site from Mashnaqa would be older than the one from Mari. The second case is around 2000 BC. Four different sites of baked brick fragments from Mari (MR02, MR03 and MR04 collected from the Great Royal Palace and MR15 from the Oriental Palace; see Table 1) provide at least two different intensity values (Fig. 8), although they are all archeologically dated at the beginning of the city 3 of Mari (~2100–1900 BC [12–14]). This difference likely indicates the occurrence of rapid intensity variations during this period which cannot be resolved due to the insufficient dating precision.

This study constitutes the direct continuation of the Le Goff and Gallet [1] paper. The analyses of more than one hundred pottery and brick fragments from Syria confirm that the intensity determination method developed with the Triaxe is particularly suitable for baked archeological materials. The good success rate in intensity determination obtained in our study, together with the rapidity of data acquisition with the Triaxe, make Mesopotamia a perfect working area for obtaining a very detailed, and probably the longest (~eight millennia) archeointensity curve.

### Acknowledgments

We are grateful to the archeologists who gave us pottery and brick fragments from Mari, Tell Masaikh, Mashnaqa, Sheikh Hamad and Shaara: Jean-Claude Margueron, Béatrice Müller-Margueron, Maria-Grazia Masetti-Rouault, Dominique Bayer, Hartmut Kühne and François Renel. Special thank to Agnès Genevey for many discussions and comments. We also thank two anonymous reviewers for their constructive comments on our manuscript. This is IPGP contribution no. 2098 and INSU no. 388.

### References

- [1] M. Le Goff, Y. Gallet, A new three-axis vibrating sample magnetometer for continuous high-temperature magnetization measurements: applications to paleo- and archeointensity determinations, *Earth Planet. Sci. Lett.* 229 (2004) 31–43.
- [2] E. Thellier, O. Thellier, Sur l'intensité du champ magnétique terrestre dans le passé historique et géologique, *Ann. Geophys.* 15 (1959) 285–376.
- [3] R. Coe, Paleo-intensities of the earth's magnetic field determined from Tertiary and Quaternary rocks, *J. Geophys. Res.* 72 (1967) 3247–3262.
- [4] A. Genevey, Y. Gallet, J. Margueron, Eight thousand years of geomagnetic field intensity variations in the eastern Mediterranean, *J. Geophys. Res.* 108 (2003) 2228, doi:10.1029/2001JB001612.

- [5] M. Boyd, A new method for measuring paleomagnetic intensities, *Nature* 319 (1986) 208–209.
- [6] H. Tanaka, J. Athanassopoulos, J. Dunn, M. Fuller, Paleointensity determinations with measurements at high temperature, *J. Geomagn. Geoelectr.* 47 (1995) 103–113.
- [7] J. Fox, M. Aitken, Cooling-rate dependence of thermoremanent magnetization, *Nature* 283 (1980) 462–463.
- [8] A. Genevey, Y. Gallet, Intensity of the geomagnetic field in Western Europe over the past 2000 years: new data from French ancient pottery, *J. Geophys. Res.* 107 (2002) 2285, doi:10.1029/2001JB000701.
- [9] A. Genevey. Apport de l'archéomagnétisme à la connaissance du champ magnétique terrestre durant les derniers millénaires, PhD Thesis, Institut de Physique du Globe de Paris (2002) 217.
- [10] D. Beyer, Evolution de l'espace bâti sur un site de la vallée du Khabur au IV millénaire. Les fouilles Françaises de Mashnaqa, in *Natural Space, Inhabited Space in Northern Syria (10th–2nd Millennium BC)*, in: M. Fortin, O. Aurenche (Eds.), *Bull.*, vol. 33, Can. Soc. for Mesopotamian Stud., Toronto Canada, 1998, pp. 139–147.
- [11] J.-Cl. Margueron, *Les Mésopotamiens*, A. and J. Picard, Paris, 2003, 447 pp.
- [12] J.-Cl. Margueron, *Mari Métropole de l'Euphrate au IIIe et au début du Iie millénaire av. J. -C.*, A. and J. Picard, Paris, 2004, 575 pp.
- [13] MARI *Annales de Recherches Interdisciplinaires*, vol. 1 to 8 (1982–1997) ERC Paris.
- [14] M.-G. Masetti-Rouault, *Rapporto preliminare degli scavi di Tell Masaikh: Il cantiere E*, Athenaeum, Studi Lett. Stor. Antich. 89 (2001) 633–638.
- [15] H. Kühne, The history of the lower Habur-region in the light of the excavations of Tell Sheikh Hamad/Dur –Katlimmu, in: F. Ismail (Ed.), *Proceedings of the International Symposium on Syria and the Ancient Near East 3000–300 BC*, Aleppo University Publications, Syria, 1995, pp. 95–123.
- [16] F. Villeneuve, *L'économie rurale et la vie des campagnes dans le Hauran antique (1<sup>er</sup> siècle av. –6<sup>e</sup> siècle ap. J.-C.)*, in: J.-M. Dentzer (Ed.), *Recherches Archéologiques sur la Syrie du Sud à l'Époque Hellénistique et Romaine*, *Inst. Fr. d'Archéol. du Proche Orient*, Damascus Syria, 1985, 218 pp.
- [17] Y. Gallet, A. Genevey, V. Courtilot, On the possible occurrence of “archeomagnetic jerks” in the geomagnetic field over the last three millennia, *Earth Planet. Sci. Lett.* 214 (2003) 237–242.
- [18] I. Snowball, P. Sandgren, Geomagnetic field intensity changes in Sweden between 9000 and 450 cal BP: extending the record of “archeomagnetic jerks” by means of lake sediments and the pseudo-Thellier technique, *Earth Planet. Sci. Lett.* 227 (2004) 361–375.